Uncovering a Shared Epitope–Activated Protein Citrullination Pathway

Vincent van Drongelen,[1] Wahida H. Ali,[1] and Joseph Holoshitz

Rheumatoid arthritis (RA) is closely associated with shared epitope (SE)–coding *HLA-DRB1* alleles and circulating anticitrullinated protein Abs (ACPA), but neither the respective pathogenic roles of SE and ACPA in RA nor the mechanisms underlying their coassociation are known. It was recently shown that the SE functions as a signal transduction ligand that activates a cell surface calreticulin-mediated, proarthritogenic, bone erosive pathway in an experimental model of RA. In this study, we demonstrate that stimulation of murine macrophages with LPS or DTT facilitated cell surface translocation of calreticulin, which in turn enabled increased SE-activated calcium signaling and activation of peptidylarginine deiminase with the resultant increased cellular abundance of citrullinated proteins. The i.p. administration of LPS to transgenic mice carrying a human SE-coding *HLA-DRB1* allele lead to increased serum levels of TNF-α and anticitrullinated cyclic peptide Abs, along with terminal phalanx bone destruction. These data uncover a previously unknown signal transduction pathway by which the SE facilitates protein citrullination, ACPA production, and bone destruction. ***The Journal of Immunology*****, 2020, 205: 579–586.**

The rheumatoid arthritis (RA) shared epitope (SE), a sequence motif in position 70–74 of the HLA-DRβ-chain is a major risk factor for RA (1, 2). Past research has demonstrated that the SE works synergistically with environmental factors (3, 4) and confers a higher risk for RA, with earlier disease onset, more severe bone erosions (5), and formation of anti–citrullinated (Cit) protein Abs (ACPA). ACPA are more commonly found in SE-positive rather than SE-negative RA patients (6), but the cause–effect basis of this association is unknown. Additionally, although ACPA have been proposed to have effector roles in RA, dysregulation of peptidylarginine deiminase (PAD) enzymes and overabundance of Cit proteins in RA tissues have been implicated as important pathogenic factors as well (7–9).

The mechanisms by which the SE affects susceptibility to RA and arthritis severity are unknown. The prevailing hypotheses postulate that the SE allows the presentation of putative self or foreign arthritogenic Ags (10) or Cit proteins (11) to T lymphocytes, which help B cells to produce autoantibodies, such as ACPA (discussed in Ref. 12); however, direct evidence to support these hypotheses is scant. We have previously shown that independent of an Ag presentation role, the SE interacts physically with cell surface calreticulin (CRT) (csCRT) and transduces intracellular signaling events, which activate Th17 polarization and osteoclast (OC) differentiation that facilitate erosive arthritis in an experimental model of RA (13–19). Based on these findings, in this study, we investigated whether the SE may contribute to the production of Cit proteins in RA through signaling events.

Materials and Methods

Reagents and cells

Fluo-4AM was purchased from Life Technologies (Eugene, OR). Linear 5-mer peptides QKRAA and DERAA as well as 15-mer peptides 65–79*0401 (KDLLEQKRAAVDTYC) and 65–79*0402 (KDILEDERAAVDTYC) were all synthesized and purified (>90%) as we previously described (17, 18). LPS was purchased from Sigma-Aldrich (Saint Louis, MO). HiPerFect Transfection Reagent and FlexiTube small interfering RNA (siRNA) oligonucleotides were purchased from QIAGEN (Valencia, CA). Protein A/G PLUS-Agarose beads (sc-2003) were purchased from Santa Cruz Biotechnology (Dallas, TX). Cl-amidine, a pan PAD inhibitor, was purchased from Calbiochem (Billerica, MA). YW3-56, a selective PAD2 and PAD4 inhibitor, was purchased from Cayman Chemical (Ann Arbor, MI). The Antibody Based Assay for PAD Activity (ABAP) assay kit was purchased from ModiQuest Research (Nijmegen, the Netherlands). The mouse macrophage RAW 264.7 cell line was purchased from American Type Culture Collection (Manassas, VA).

Abs

Mouse monoclonal pan citrullination Ab (MABN328) was purchased from MilliporeSigma (Billerica, MA) and used for immunoblotting of Cit proteins. Mouse polyclonal pan citrullination Ab (ab6464) was purchased from Abcam (Cambridge, MA) and used for immunoprecipitation. Mouse polyclonal anti–α-enolase (no. 3810) and monoclonal antivimentin (no. 5741) Abs were purchased from Cell Signaling Technology (Danvers, MA). Mouse anti–β-actin (BA3R, MA5-15739) mAb was purchased from Thermo Fisher Scientific (Waltham, MA). ECL HRP-conjugated anti-mouse (NA931VS) and anti-rabbit (N934V) Abs were purchased from Amersham via GE Healthcare Lifesciences (Chicago, IL).

Department of Internal Medicine, University of Michigan School of Medicine, Ann Arbor, MI 48109

[1]V.v.D. and W.H.A. are equal contributors.

ORCID: 0000-0003-0196-8040 (W.H.A.).

Received for publication September 11, 2019. Accepted for publication May 26, 2020.

This work was supported by the Rheumatology Research Foundation of the American College of Rheumatology and by National Institutes of Arthritis and Musculoskeletal and Skin Diseases Grants R01 AR059085, R01 AR073014, and R33 AR074930 (to J.H.) and T32 AR07080 (to W.H.A.).

V.v.D. and W.H.A. designed and conducted the experiments and wrote the manuscript. J.H. conceptualized and oversaw the project and edited the manuscript.

Address correspondence and reprint requests to Dr. Vincent van Drongelen, University of Michigan School of Medicine, MSRB 1 Room 5514, SPC 5680, 1150 West Medical Center Drive, Ann Arbor, MI 48109-5680. E-mail address: vvincent@med.umich.edu

The online version of this article contains supplemental material.

Abbreviations used in this article: ACPA, anti-Cit protein Ab; BAPTA-AM, 1,2-bis(*o*-aminophenoxy) ethane-*N*,*N*,*N*′,*N*′-tetraacetic acid; BMDM, bone marrow–derived macrophage; CIA, collagen-induced arthritis; Cit, citrullinated; CRT, calreticulin; csCRT, cell surface CRT; ER, endoplasmic reticulum; micro-CT, micro computed tomography; MS, mass spectrometry; MS1, first-stage MS; OC, osteoclast; PAD, peptidylarginine deiminase; RA, rheumatoid arthritis; SE, shared epitope; siRNA, small interfering RNA; Tg, transgenic.

Mice

Transgenic (Tg) mice, expressing cell surface human HLA-DR molecules containing the β-chains coded by SE-positive *HLA-DRB1*04:01* or SE-negative *HLA-DRB1*04:02* alleles (20, 21), were kindly provided by Dr. C. David at the Mayo Clinic and are referred to as Tg 0401 and Tg 0402, respectively. Experiments were carried out in 10–12-wk-old female mice and housed in a specific pathogen-free, temperature-controlled room (25°C) with a 12-h dark and 12-h light cycle. All protocols for mouse experiments were approved by the University of Michigan Unit for Laboratory Animal Medicine and by the University of Michigan Committee on Use and Care of Animals. Mice were maintained in accordance with all applicable federal, state, local, and institutional laws, regulations, policies, principles, and standards governing animal research.

Cell cultures

RAW 264.7 macrophages were cultured in DMEM medium supplemented with 10% heat-inactivated FBS and 5% penicillin/streptomycin. Cells were grown in T75 flasks to confluence and split every 3 d. Cells were used between passage 6 and 10. Bone marrow cells were collected from femurs of age-matched SE-positive and SE-negative female mice and plated in deep, nontissue culture-treated petri dishes. Bone marrow–derived macrophages (BMDM) were differentiated using L929 cell conditioned media for 6 d (10% FBS, 1% penicillin/streptomycin, and 30% L929 cell conditioned media in DMEM supplemented with 0.5% pyruvate). Medium was changed on day 3. Mature BMDM were split on day 5 and seeded at appropriate concentrations for experiments.

Intracellular calcium measurement

RAW 264.7 macrophages were seeded at 5×10^4 cells/well in 48-well plates overnight. Cells were washed once with PBS, followed by incubation with 4 μM Fluo-4 in PBS at 37°C for 30 min. To increase dye access into macrophages, Fluo-4AM was dissolved in pluronic acid (Invitrogen). Excess dye was removed, and cells were washed once with PBS. Samples were then treated with 1 μg/ml LPS or 2 mM DTT in PBS and incubated at 37°C for 45 min. Macrophages were then equilibrated at room temperature for 15 min. Baseline fluorescence was measured (excitation 488 nm, emission 516 nm, time point = before experiment) using a Synergy H1 Hybrid Reader (BioTek Instruments). Then, 15-mer or 5-mer peptides were added. Fluorescence was measured every 5 min for 60 min. For BMDM, experiments were conducted as above, except measurements were collected during LPS treatment.

In some experiments, brefeldin A (10 μM; Sigma) was added to cell culture media 1 h prior to Fluo-4 incubation. In other experiments, cell-permeable calcium chelator 1,2-bis(*o*-aminophenoxy) ethane-*N*,*N*,*N*′,*N*′-tetraacetic acid (BAPTA-AM, 2.5 μM; Invitrogen) was added 15 min prior to the addition of peptides. In knockdown experiments, siRNA was incubated with cells for at least 24 h prior to Fluo-4 addition.

PAD activity assay

Samples were lysed using PAD lysis buffer (20 mM Tris-HCl, 10 mM 2-ME, 100 mM NaCl, 10% glycerol, and EDTA-free protease inhibitor) followed by sonication and removal of cell debris by centrifugation. The ABAP assay (22) was performed according to manufacturer's instructions, with the exception that it was performed using calcium-free buffers only. To this end, samples were loaded in lysis buffer without the manufacturer's calcium-containing buffers. Additionally, following incubation with deamination buffer and prior to the addition of samples, wells were washed three times with TBST and twice with TBS to remove excess calcium. This modification was done to prevent the constitutive activation of PAD while allowing the determination of inducible PAD activity only.

Crt knockdown

For *Crt* knockdown, we used siRNA against either mouse Calr3 (NM_028500 and NM_029782; QIAGEN) or a negative control siRNA (AllStars; QIAGEN). siRNA oligonucleotides were complexed with HiPerFect Transfection Reagent in Opti-MEM at a 1:6 ratio. Vesicles were added to RAW 264.7 macrophages at least 24 h prior to use. The knockdown efficiency was determined by RT-PCR and was 30%.

Protein analysis

To measure Cit proteins, cells were seeded in six-well plates at a concentration of 1×10^6 cells/well in the presence or absence of 100 ng/ml of LPS or 500 μM of DTT and in the presence or absence of 100 μg/ml of SE 15-mer peptide. In some experiments, BAPTA-AM (2.5 mM, Invitrogen) or PAD inhibitors (Cl-amidine, 5.7 mM, or YW3-56, 1 mM) were added to cell culture media 1 h prior to LPS and/or 15-mer addition. Cells were incubated at 37°C for 16 h and then collected in cold PBS, pelleted, and frozen at −20°C. Pellets were resuspended in radioimmunoprecipitation assay buffer (RIPA buffer, Sigma), and protein concentration was measured by Detergent Compatible Assay (Bio-Rad Laboratories). Citrullination was determined either by immunoblotting or tandem liquid chromatography–mass spectrometry (MS) (Supplemental Fig. 1F, Supplemental Table I).

Immunoblotting

To detect total protein citrullination, 150 μg of protein were separated using a Novex 4–20% Tris-Glycine Gel and transferred onto a nitrocellulose membrane. Anticitrullination Ab (MABN328) was used to probe for Cit proteins. All Abs were diluted 1:1000 in 5% BSA in TBST and incubated with the membrane at 4°C overnight. Membranes were then washed three times with TBST followed by incubation with the appropriate secondary Ab (1:10,000) for 1 h at room temperature. Chemiluminescence (WesternBright ECL; Advansta) was visualized using Omega Lum C software. Membranes were then stripped using Restore Stripping Buffer (Thermo Fisher Scientific) according to the manufacturer's protocol and reprobed using an anti-actin Ab (BA3R, 1:2500) for 1 h at room temperature. Quantitation of protein band abundance was performed using ImageJ software. Quantification of Cit proteins were normalized to actin.

Confocal microscopy

To stain for csCRT, nonpermeabilized cells, as previously described (23), were stained with anti-CRT Ab (PA3-900) diluted 1:100, followed by a secondary FITC-labeled anti-rabbit Ab (sc-2012). Excess Abs were removed between each step by PBS. Coverslips were mounted using VECTASHIELD with DAPI. Confocal images were acquired at room temperature on a Leica SP5× Inverted Two-Photon Fluorescence-Lifetime Imaging Microscopy Confocal using a 63× objective.

Mass spectroscopy of Cit proteins

Immunoprecipitated Cit protein bands (Supplemental Fig. 1E) were excised, and gel slices were destained with 30% methanol for 4 h. Proteins were digested overnight with a sequencing-grade, modified trypsin (Promega). The tryptic digests were resolved on a nano-capillary reverse phase column (Acclaim PepMap C18, 2 μm, 25 cm; Thermo Fisher Scientific) using a 1% acetic acid/acetonitrile gradient at 300 nl/min and directly introduced to Orbitrap Fusion Tribrid Mass Spectrometer (Thermo Fisher Scientific, San Jose, CA). First-stage MS (MS1) scans were acquired at 120 K resolution. Data-dependent high-energy C-trap dissociation tandem MS spectra were acquired with a top speed option (3 s) following each MS1 scan (relative capillary electrophoresis~32%). Proteins were identified by searching the data against the *Mus musculus* database (UniProtKB) using Proteome Discoverer (v1.4; Thermo Fisher Scientific). Search parameters included MS1 mass tolerance of 10 ppm and fragment tolerance of 0.2 Da, and two missed cleavages were allowed; carbamidomethylation of cysteine was considered fixed modification, and oxidation of methionine and citrullination of arginine were considered as potential modifications. Percolator algorithm was used for discriminating between correct and incorrect spectrum identification. The false discovery rate was calculated at the peptide level, and peptides with <1% false discovery rate were retained. Once analyzed by the software, the top 10% of hits were reviewed manually. Only peptides that possessed the mass shift and an arginine that could be Cit were considered validated.

In vivo experiments

The i.p. injections of either PBS or LPS (50, 250, or 500 μg/kg) were performed in 12-wk-old female Tg 0401 and Tg 0402 mice. For long-term experiments, mice were injected once every 7 d for 42 d. Final injections were performed on day 42, 4 h prior to sacrifice, at which time serum and limbs were collected for analysis. Serum was analyzed using ELISA for TNF-α (R&D Systems), total IgG (Innovative Research), and anti-CCP (TSZ ELISA, no. M1188), according to the manufacturer's protocol, and for PAD activity using the ABAP assay as described above. Limbs were used to determine bone erosion via x-ray and micro computed tomography (micro-CT) scans.

Bone imaging

Radiographs were taken using a microradiography system (Faxitron, Wheeling, IL) with the following operating settings: 27 peak voltage, 2.5 mA anode current, and an exposure time of 4.5 s. Coded radiographs were evaluated blindly. Rear paw terminal phalanx osteolysis were scored based on the number of affected digits on a 0–10 scale.

For micro-CT, limbs were dissected, fixed in 10% formalin, and stored in 70% ethanol. Limbs were scanned ex vivo by a micro-CT system (eXplore Locus SP; GE Healthcare Pre-Clinical Imaging, London, ON, Canada) in distilled water. The protocol included a source powered at 80 kV and 80 μA. In addition to a 0.508-mm AL filter, an acrylic beam flattener was used to reduce the beam-hardening artifact. Exposure time was defined at 1600 ms/frame with 400 views taken at increments of 0.5˚. With four frames averaged and binning at 2 × 2, the images were reconstructed with an 18-μm isotropic voxel size.

Statistics

Unless otherwise specified, unpaired *t* tests, assuming Gaussian distribution, with Welch correction were used to measure significance. Holm–Sidak method (each row analyzed individually, not assuming consistent SD, $\alpha = 5\%$) was used to determine significance in calcium signaling experiments. Significance is depicted in figures as follows: $*p < 0.05$, $**p < 0.01$, $***p < 0.001$, and $****p < 0.0001$.

Results

The SE ligand activates protein citrullination in vitro

We have previously demonstrated that synthetic 15-mer and 5-mer peptides that express the SE sequence motif act as signal transduction ligands that interact with csCRT and activate a pro-osteoclastogenic pathway (13–19). To investigate whether the SE ligand may be directly involved in protein citrullination, in this study, we first examined the ability of 5-mer and 15-mer peptides that express a *DRB1*04:01*-coded SE motif QKRAA to increase intracellular calcium. To optimize the conditions for interaction between the SE ligand and its receptor csCRT, mouse RAW 264.7 macrophages were pretreated with LPS or DTT, which are known to induce endoplasmic reticulum (ER) stress, leading to translocation of CRT to the cell surface (24–27). Indeed, RAW 264.7 macrophages treated with either LPS or DTT did display increased csCRT as did, to a lesser extent, those that were treated with the 15-mer SE ligand alone (Supplemental Fig. 1A). Increased expression of csCRT enabled SE ligand-activated intracellular calcium increase (Fig. 1A–D). When applied alone, neither LPS (Fig. 1A) nor DTT (Fig. 1B) could activate calcium signaling, suggesting that cross-talk between the SE and the ER stressor pathways is required. The signal was sequence specific as it could be induced only by peptides containing the SE motif (Fig. 1C, 1D) and was SE ligand dose-dependent with an EC_{50} = 336.2 μM (Supplemental Fig. 1B, 1C). We also confirmed that SE-activated signaling was csCRT dependent because inhibition of Crt translocation (Fig. 1E, Supplemental Fig. 1D) or *Crt* silencing (Fig. 1F) blocked the signal. Together, these findings indicate that ligand–receptor interaction between the SE and csCRT activates intracellular calcium signaling.

We next examined whether SE ligand-activated calcium signaling leads to increased PAD activity. To determine enzymatic activity in response to treatment rather than a reflection of PAD enzyme abundance, we measured the activity in the absence of exogenous calcium, using calcium-free buffers for lysis and assays. LPS-pretreated RAW 264.7 macrophages stimulated with the 15-mer peptide showed a significant immediate (within 1 h) increase in PAD activity (Fig. 2A). LPS and SE ligand alone also tended to increase PAD activity, but these did not reach statistical significance. Following an overnight incubation of RAW 264.7 cells with LPS plus the SE 15-mer peptide, a significant increase in protein citrullination was observed (Fig. 2B, 2C). The citrullination

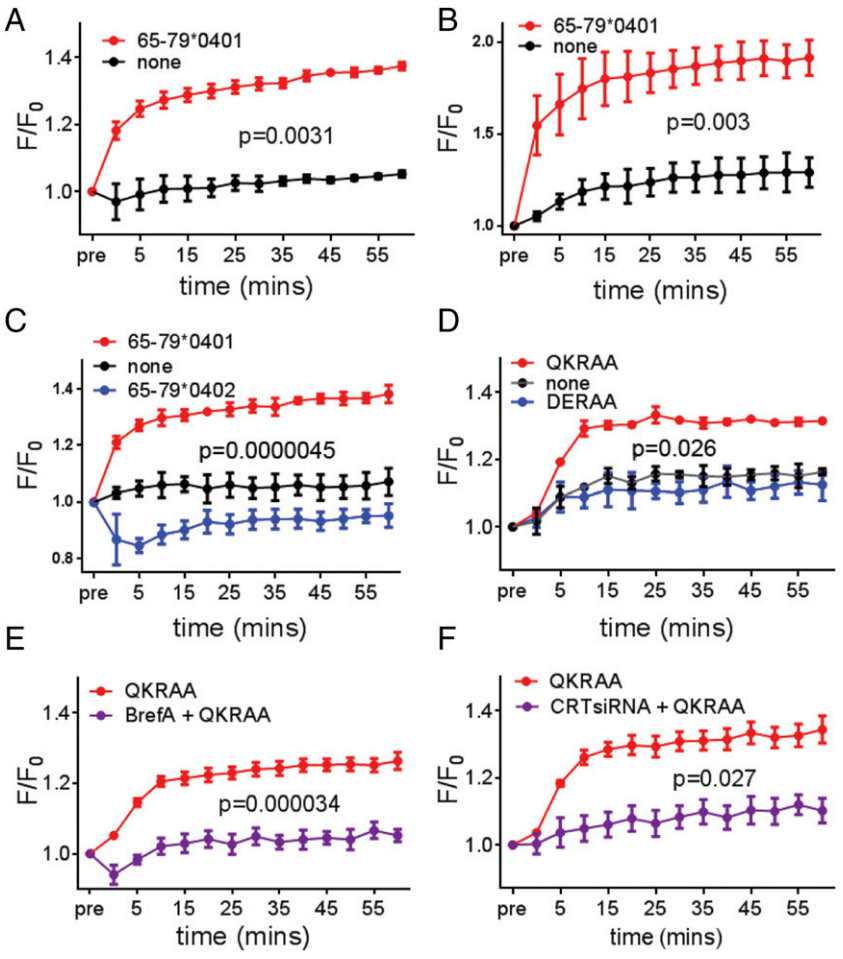

FIGURE 1. Synthetic SE ligands increase intracellular calcium in RAW 264.7 macrophages. Cells were pretreated for 1 h with LPS [1 μg/ml, (**A**)] or DTT [2 mM, (**B**)] without (none) or with the subsequent adding of 400 μg/ml of a 15-mer SE ligand (65–79*0401), and intracellular calcium was measured over time. (**C** and **D**) Cells were pretreated for 1 h with LPS (1 μg/ml), followed by adding 400 μg/ml 15-mer SE ligand (65–79*0401) or SE negative (65–79*0402) (C) or 2.5 μg/ml 5-mer SE ligand (QKRAA) or SE-negative peptide (DERAA) (D). (**E** and **F**) Cells were pretreated with brefeldin A (BrefA, 10 μM, 1 h) (E) or transfected with CRT siRNA (F) followed by LPS and 2.5 μg/ml 5-mer SE ligand (QKRAA) followed by intracellular calcium measurement over time. Data represent mean ± SEM of fluorescence/initial fluorescence (F/F_0) from three (A–D) or two (E and F) independent experiments with four biologic replicates in each.

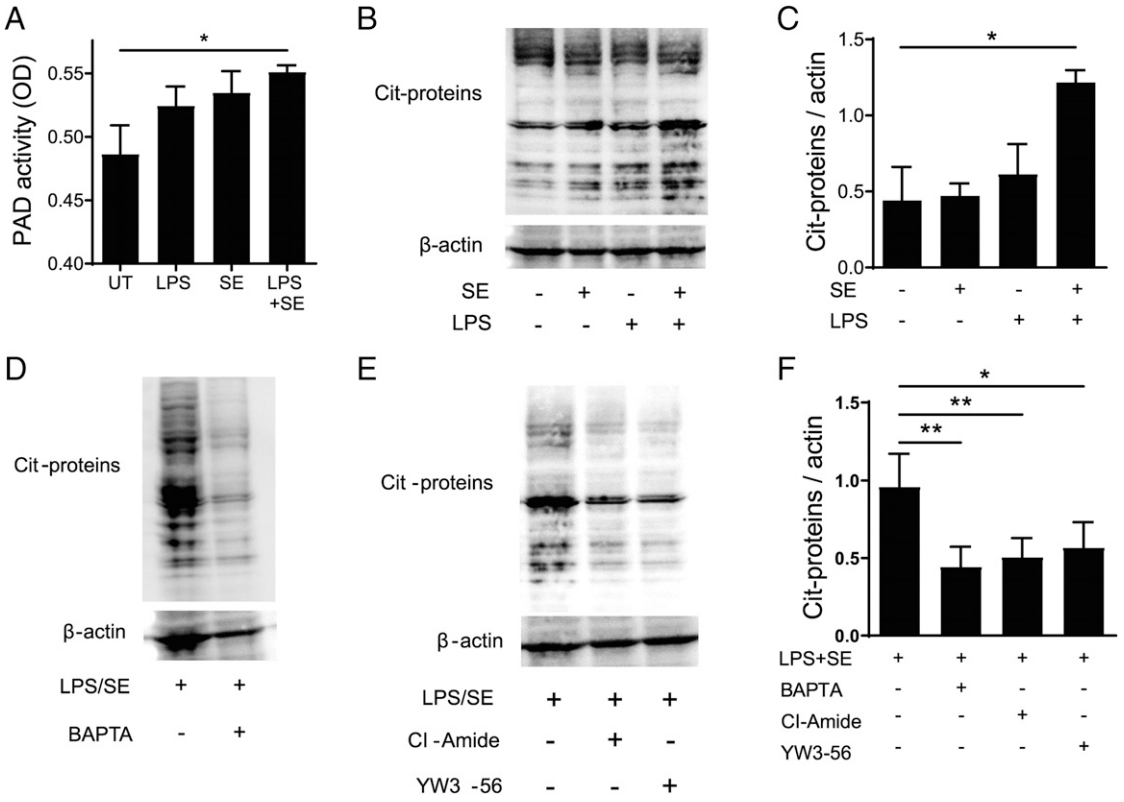

FIGURE 2. Synthetic SE ligand increases protein citrullination in RAW 264.7 macrophages. (**A**) PAD activity in cells stimulated for 1 h with or without LPS 1 μg/ml in the presence or absence of SE 15-mer peptide (400 μg/ml). (**B**) Cit proteins in cells incubated overnight with or without LPS (100 ng/ml) in the presence or absence of 15-mer SE ligand (100 μg/ml). (**C**) Quantitation of Cit proteins normalized to β-actin from three independent experiments as in (B). (**D**) Cells stimulated overnight with LPS (100 ng/ml) and 15-mer SE ligand (100 μg/ml) with or without a calcium chelator (BAPTA-AM). (**E**) Cells stimulated as in (D) with or without PAD inhibitors (Cl-amidine, middle lane; YW3-56, left lane). (**F**) Quantitation of Cit proteins normalized to β-actin from three independent experiments as in (E). Quantification data in (C) and (F) represent mean and SD from three independent experiments. $*p < 0.05$, $**p < 0.01$.

was dependent on calcium and PAD activity because a calcium chelator (BAPTA-AM) as well as inhibition of PAD by Cl-amidine (a pan PAD inhibitor) or YW3-56 (a PAD2- and PAD4-selective inhibitor) reduced the levels of protein citrullination (Fig. 2D–F). MS analysis identified citrullination of several proteins, including some that have been previously shown to be targeted by ACPA in RA (28, 29), such as vimentin, α-enolase, histones, and actin (Supplemental Table I). The identity of two Cit proteins, α-enolase and vimentin, and the involvement of PAD and calcium in the process was confirmed by immunoblotting (Supplemental Fig. 1F). Thus, taken together, these data indicate that the SE increases cellular protein citrullination through a calcium-dependent PAD activation pathway.

Ex vivo effects of constitutively expressed SE in HLA-DR humanized mice

To determine whether the SE has similar effects in its intact cell surface conformation, we studied ex vivo BMDM from humanized mice with the cell surface expression of functional SE-positive HLA-DR molecules coded by the human *HLA-DRB1*04:01* allele (Tg 0401). As a control, we used BMDM from Tg 0402 mice carrying the SE-negative allele *HLA-DRB1*04:02*, which codes for a DRβ-chain that differs from the one coded by the **04:01* allele by only 3 aa residues in the third allelic hypervariable region (residues 65–79) (20, 21).

Consistent with the in vitro findings above, BMDM from Tg 0401 mice, which constitutively express the SE in its natural conformation, responded to LPS treatment by increasing intracellular calcium signaling (Fig. 3A). Tg 0401 BMDM also demonstrated significantly higher constitutive PAD activity, which increased significantly upon stimulation with LPS (Fig. 3B), as well as increased constitutive expression of csCRT (Fig. 3C) and Cit protein abundance (Fig. 3D, 3E) as compared with BMDM from Tg 0402. These findings demonstrate the impact of csCRT expression levels on PAD enzymatic activity and the abundance of Cit proteins ex vivo. Furthermore, LPS stimulation produced a significantly higher release of TNF-α in Tg 0401 BMDM compared with Tg 0402 BMDM (Fig. 3F).

In vivo SE effects in HLA-DR humanized mice

To investigate this pathway in vivo, Tg 0401 and Tg 0402 mice received weekly i.p. injections of either 250 μg/kg LPS or PBS for six consecutive weeks. There was no clinical or radiographic evidence of arthritis (data not shown); however, 6/10 LPS-treated SE-positive Tg 0401 mice developed terminal phalanx swelling (Fig. 4A). In contrast, only 2/10 Tg 0401 mice treated with PBS and 0/20 SE-negative Tg 0402 mice treated with either PBS or LPS displayed such swelling (Fig. 4A). When paws were examined radiographically, Tg 0401 mice treated with LPS displayed terminal phalanx osteolysis (Fig. 4B). Histological examination revealed terminal phalanx bone destruction (Fig. 4C). Comparable radiologic findings were seen in mice treated as above with low-dose (50 μg/kg) LPS (Supplemental Fig. 2A).

Serum IgG increased equally in SE-positive Tg 0401 and SE-negative Tg 0402 mouse lines in response to LPS (Supplemental Fig. 2B). However, Tg 0401 mice developed significantly higher serum TNF-α levels (Fig. 4D), PAD activity (Fig. 4E),

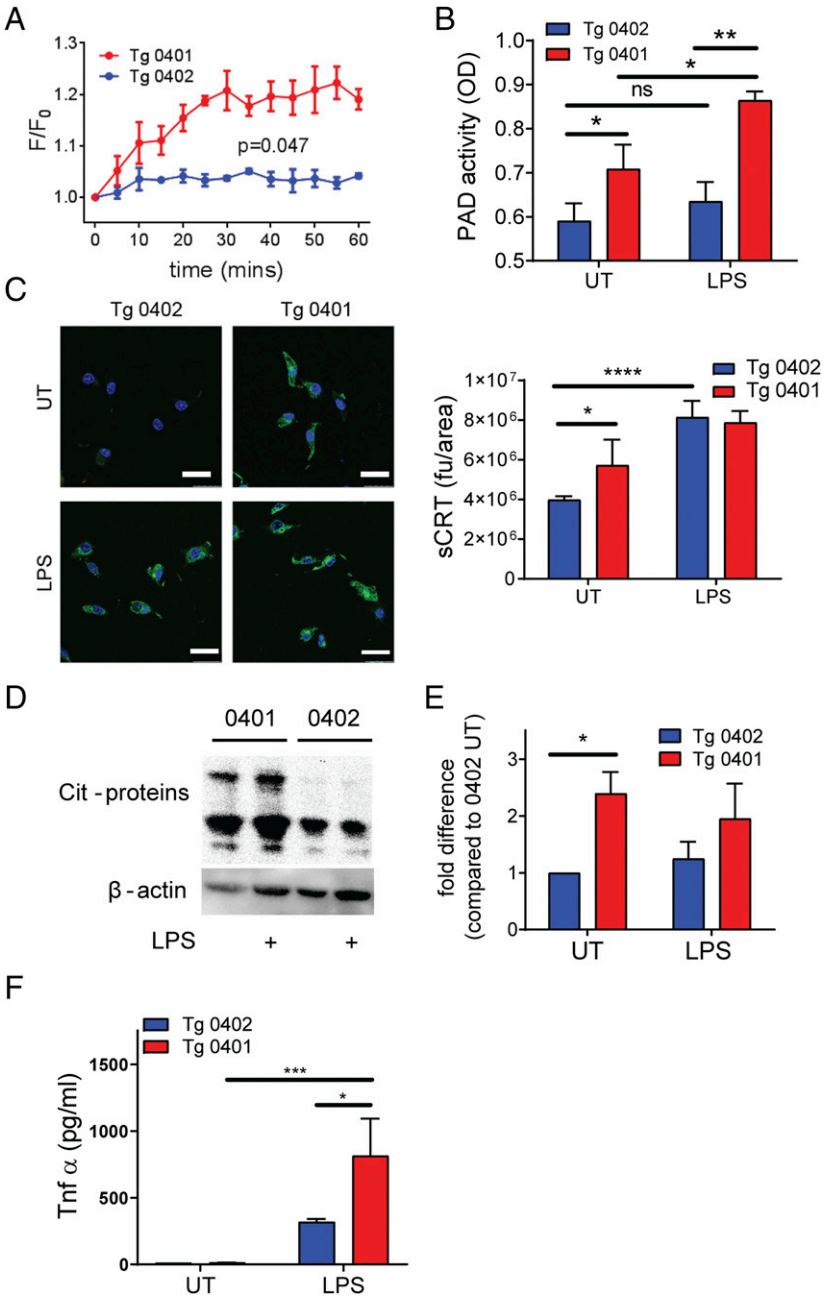

FIGURE 3. Protein citrullination by endogenous SE in BMDM. (**A**) Intracellular calcium in LPS-treated (1 μg/ml, 1 h) BMDM from SE-negative (Tg 0402) or SE-positive (Tg 0401) mice. Mean + SEM from three independent experiments with six biologic replicates in each. (**B**) PAD activity in untreated (UT) or LPS-treated (1 μg/ml, 1 h) BMDM. (**C**) csCRT (green) in UT or LPS -treated (1 μg/ml, 1 h) BMDM. Scale bar, 10 μm. Mean + SD of three confocal experiments, five fields/experiment. (**D**) Anti–Cit protein immunoblots of BMDM protein extracts from SE-positive and SE-negative mice stimulated with or without LPS. (**E**) Quantitation of total Cit proteins normalized to β-actin. Mean ± SD of four independent experiments. $*p < 0.05$, $**p < 0.01$, $****p < 0.0001$. (**F**) TNF-α secretion by BMDM stimulated with or without LPS for 24 h. Mean + SD of three independent experiments; one-way ANOVA. $*p < 0.05$, $***p < 0.001$.

and anti-CCP Ab levels (Fig. 4F) compared with the Tg 0402 mice. Increased anti-CCP Abs in these mice was LPS dose dependent (Supplemental Fig. 2C). Thus, when exposed to LPS, SE-positive mice develop higher TNF-α levels, PAD activity, anti-CCP Ab production, and bone erosion. We included a summary of these findings in a proposed model (Fig. 5).

Discussion

SE-coding *HLA-DRB1* alleles and ACPA have long been found to coassociate with RA, but the underlying mechanism for their coassociation is currently unknown. Although studies by others have demonstrated increased calcium-dependent PAD expression in RA synovial macrophages with the resultant increased protein citrullination (30), the role of the SE in this process has not been investigated. Based on our previous findings that the SE acts as a signal transduction ligand that activates proarthritogenic bone-destroying pathways upon interaction with csCRT (13–19), in this study, we sought to determine whether the SE ligand can activate a protein citrullination signaling pathway.

The findings presented in this study uncovered a signal transduction pathway by which the SE facilitates protein citrullination, ACPA production, and extra-articular bone destruction. To our knowledge, these findings indicate, for the first time, a signaling pathway-based mechanism for SE–ACPA association. The prevailing hypothesis concerning this association postulates that the SE allows HLA-DR molecules to present Cit proteins to T lymphocytes, with the resultant stimulation of B cells to produce ACPA (11). However, that hypothesis does not address substantial evidence implicating dysregulated PAD enzymes and the overabundance of Cit proteins as important pathogenic factors in RA (7–9).

We have previously demonstrated higher ex vivo rates of OC differentiation and bone degradation activity in bone marrow cells derived from SE-expressing Tg 0401 mice (15). Furthermore, cell-free synthetic SE ligands facilitated arthritis and articular bone damage in mice with collagen-induced arthritis (CIA) (14, 15).

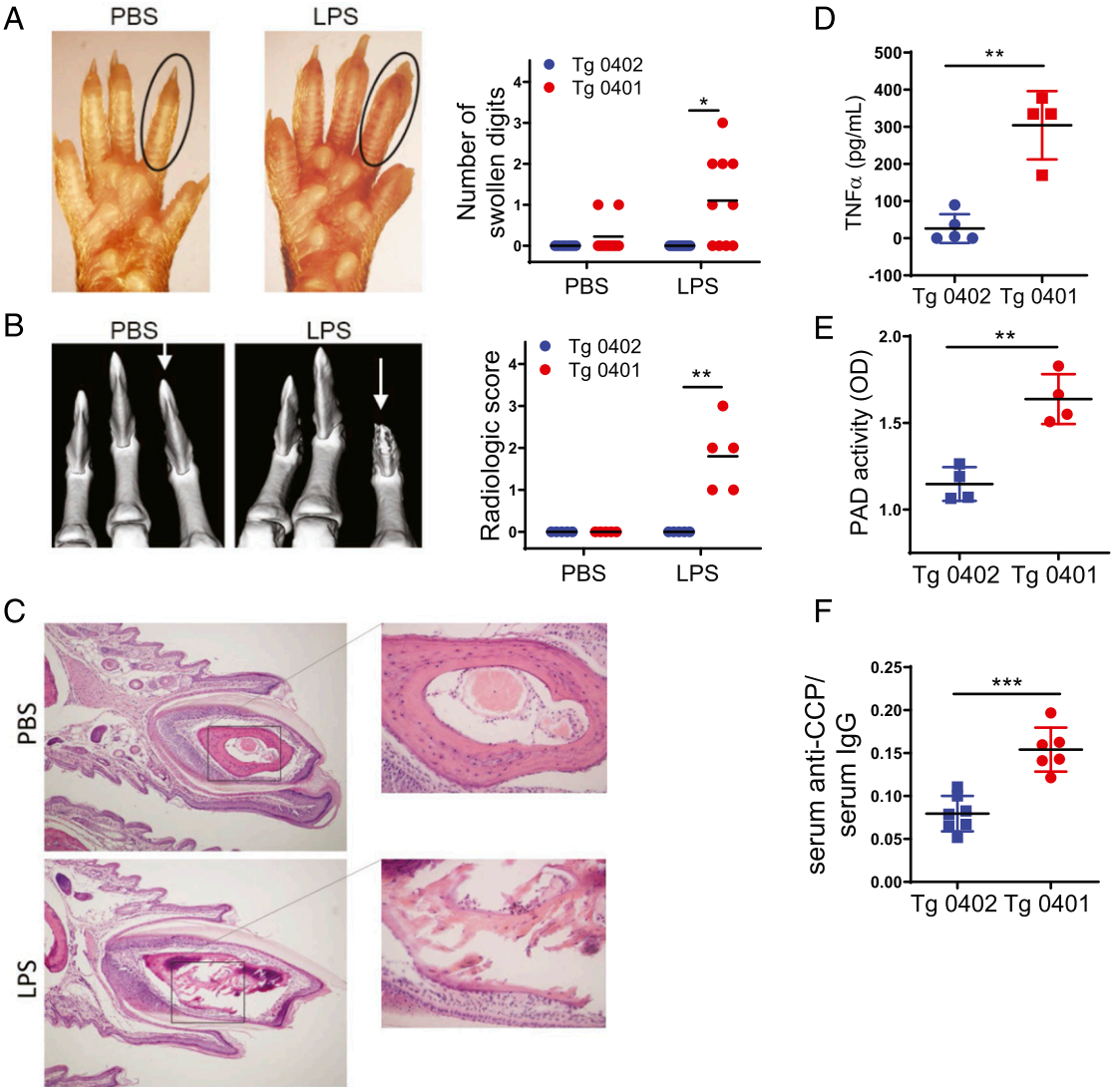

FIGURE 4. SE effects in vivo. (**A**) Representative paw images of PBS- (left) or LPS- (right) treated Tg 0401 mice. The graph on the right depicts the number of swollen digits in mice given 6 wk i.p. injections of PBS or LPS (250 μg/kg). Cumulative data from two independent experiments. (**B**) Micro-CT images of digits from mice treated as in (A). The graph on the right depicts the radiologic scores. (**C**) H&E staining of a representative rear paw terminal phalanx from Tg 0401 mice PBS treated (top) or LPS treated (bottom) as in (A). Original magnification ×10; inset: original magnification ×40. (**D**) Serum TNF-α levels 4 h following the administration of the final LPS (500 μg/kg) dose of a 6-wk course. TNF-α was undetectable in PBS-treated mice. (**E**) Serum PAD activity in mice injected with LPS as in (A), relative to sera of PBS-treated mice. (**F**) Circulating anti-CCP Ab levels relative to serum IgG levels of mice treated as in (A). $^{*}p < 0.05$, $^{**}p < 0.01$, $^{***}p < 0.001$.

In the current study, interestingly, upon exposure to LPS, unimmunized Tg 0401 mice showed peculiar erosive bone damage. Different from CIA mice, the erosive changes observed in this study spared the joints themselves and affected selectively an extra-articular bone site, the distal phalanges. The lack of arthritis could be explained by the fact that different from CIA, the mice studied in this study were not immunized with a joint-enriched Ag (collagen type II); however, the reason for the selective effect on the distal phalanges remains unclear. A possible explanation could be related to mechanical damage due to terminal phalanges being subject to repetitive injury in rodents. In this context, it should be mentioned that spontaneous extra-articular bone damage has been previously reported in SE-positive Tg mice (31). It is also a known feature in RA (32), and although uncommon, selective terminal phalanx osteolysis without joint involvement has been previously reported in RA as well (33).

The finding that anti-CCP Abs in LPS-treated Tg 0401 mice were associated with extra-articular bone destruction is consistent with previous reports that anti–Cit-vimentin Abs activate human and mouse OC and cause extra-articular bone damage in mice (34). Interestingly, in that study, the bone-destroying effect of ACPA was TNF-α dependent, reminiscent of the association among anti-CCP Abs, bone destruction, and high TNF-α levels demonstrated in this study. It should be cautioned, however, that despite the intriguing parallels between that study and our findings, further research is required to determine the antigenic specificity of anti-CCP Abs in LPS-treated Tg 0401 mice and whether these Abs are directly involved in acro-osteolysis.

Consistent with our previous studies (13–19), QKRAA, a core 5-mer amino acid sequence corresponding to the region 70–74 of SE-expressing HLA-DRβ-chains, was found to be essential and sufficient for activating the pathway, thereby corroborating our previous conclusion about the role of the SE as a structurally defined signal transduction ligand. It should be added, however, that others have suggested that in addition to the 5 aa residues in position 70–74, residue 11, located in the "floor" of the HLA-DR

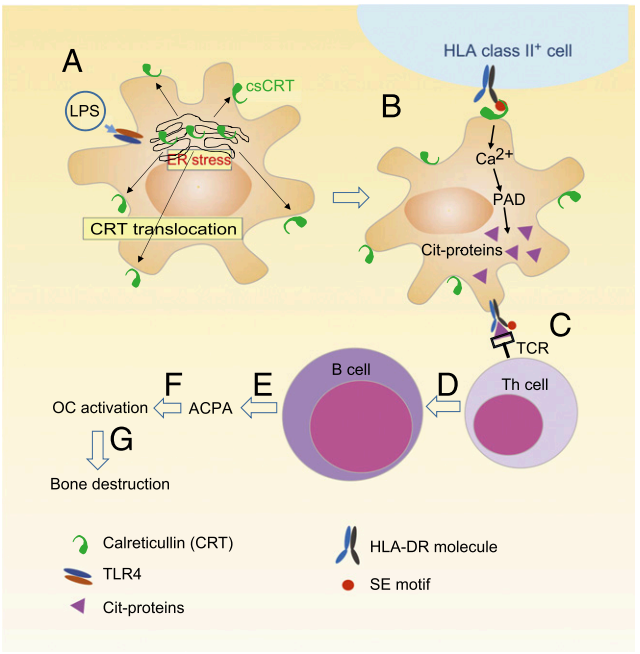

FIGURE 5. A proposed model. Based on the findings in this study and based on research reported by others, we propose the following: in SE-negative conditions (**A**), ER stress secondary to, for example, exposure to LPS triggers CRT translocation to the cell surface. In SE-positive subjects (**B**), interaction between the SE ligand and csCRT causes cellular calcium (Ca^{2+}) increase, PAD activation, and enhanced protein citrullination. SE-positive class II molecules present Cit proteins to helper T cells (**C**), as suggested by others (11), which in turn facilitate the production of ACPA by B cells (**D** and **E**). Certain ACPA, such as anti–Cit-vimentin Abs, activate OC (**F**), which facilitate bone erosion (**G**). In inflammatory arthritis, intra-articular production of TNF-α leads to the activation of the SE–csCRT pathway inside the joint cavity with resultant erosive arthritis. In the absence of arthritis, the process could affect extra-articular bone tissues, such as terminal phalanges.

peptide-binding groove, associates with RA risk as well (35), suggesting that Ag presentation is involved. However, the role of residue 11, which is based strictly on imputation of genomics data, has not been yet functionally validated, and its relevance to RA pathogenesis has been questioned (36). Be that as it may, we believe that the SE ligand effect uncovered by us and Ag presentation are mutually nonexclusive, as previously discussed (37, 38). It is not inconceivable that residues 11 and the SE region could play complementing pathogenic roles. It is also possible that whereas residue 11 plays a role in RA risk, the SE plays a dual role in both susceptibility and pathogenesis. These questions deserve experimental examination.

Based on the findings in this study and research reported by others, we propose a model of SE-associated ACPA (depicted graphically in Fig. 5). The SE was previously identified as a signal transduction ligand that facilitates erosive arthritis in mice, independent of its purported role in Ag presentation. In this study, we show that upon exposure to LPS, the SE–CRT signaling pathway facilitates calcium-dependent protein citrullination in tissue culture conditions. In vivo, this pathway activates TNF-α production, anti-CCP formation, and terminal phalanx bone destruction. Together with the previous reports that showed that the SE induced OC activation and innate signaling events, the results presented in this study show an additional RA-relevant signaling pathway that is activated by the SE, consolidating the notion that the SE acts as a signaling ligand.

It should be added that this study represents a case of interaction between genetic (SE) and environmental (LPS) factors, consistent with previous indications that bacterial Ags such as LPS may play an immune stimulatory role and facilitate autoimmune conditions, including inflammatory arthritis (39–41).

In summary, the pathway uncovered in this study illuminates a previously unrecognized functional role of the SE and could provide an experimental model to explore the role of MHC gene products in the pathogenesis of inflammatory arthritis. Whether a similar mechanism is responsible for facilitating ACPA generation in humans carrying SE-coding *HLA-DRB1* alleles and whether such a mechanism plays a role in human RA disease pathogenesis remains to be determined.

Acknowledgments

We thank Ying Liu and Xavier J. E. Owens for technical assistance.

Disclosures

J.H. is an Inventor of Regents of the University of Michigan–owned technologies, which are licensed to Zydus Cadila and Alibion. He is a consultant and holds a 2.5% equity option with Alibion. The other authors have no financial conflicts of interest.

References

1. Gregersen, P. K., J. Silver, and R. J. Winchester. 1987. The shared epitope hypothesis. An approach to understanding the molecular genetics of susceptibility to rheumatoid arthritis. *Arthritis Rheum.* 30: 1205–1213.
2. McInnes, I. B., and G. Schett. 2011. The pathogenesis of rheumatoid arthritis. *N. Engl. J. Med.* 365: 2205–2219.
3. Fu, J., S. V. Nogueira, V. V. Drongelen, P. Coit, S. Ling, E. F. Rosloniec, A. H. Sawalha, and J. Holoshitz. 2018. Shared epitope-aryl hydrocarbon receptor crosstalk underlies the mechanism of gene-environment interaction in autoimmune arthritis. *Proc. Natl. Acad. Sci. USA* 115: 4755–4760.
4. Padyukov, L., C. Silva, P. Stolt, L. Alfredsson, and L. Klareskog. 2004. A gene-environment interaction between smoking and shared epitope genes in HLA-DR provides a high risk of seropositive rheumatoid arthritis. *Arthritis Rheum.* 50: 3085–3092.
5. Gonzalez-Gay, M. A., C. Garcia-Porrua, and A. H. Hajeer. 2002. Influence of human leukocyte antigen-DRB1 on the susceptibility and severity of rheumatoid arthritis. *Semin. Arthritis Rheum.* 31: 355–360.
6. Huizinga, T. W., C. I. Amos, A. H. van der Helm-van Mil, W. Chen, F. A. van Gaalen, D. Jawaheer, G. M. Schreuder, M. Wener, F. C. Breedveld, N. Ahmad, et al. 2005. Refining the complex rheumatoid arthritis phenotype based on specificity of the HLA-DRB1 shared epitope for antibodies to citrullinated proteins. *Arthritis Rheum.* 52: 3433–3438.
7. Andrade, F., E. Darrah, M. Gucek, R. N. Cole, A. Rosen, and X. Zhu. 2010. Autocitrullination of human peptidyl arginine deiminase type 4 regulates protein citrullination during cell activation. *Arthritis Rheum.* 62: 1630–1640.
8. Giles, J. T., J. Fert-Bober, J. K. Park, C. O. Bingham, III, F. Andrade, K. Fox-Talbot, D. Pappas, A. Rosen, J. van Eyk, J. M. Bathon, and M. K. Halushka. 2012. Myocardial citrullination in rheumatoid arthritis: a correlative histopathologic study. *Arthritis Res. Ther.* 14: R39.
9. Suzuki, A., R. Yamada, and K. Yamamoto. 2007. Citrullination by peptidylarginine deiminase in rheumatoid arthritis. *Ann. N. Y. Acad. Sci.* 1108: 323–339.
10. Hammer, J., F. Gallazzi, E. Bono, R. W. Karr, J. Guenot, P. Valsasnini, Z. A. Nagy, and F. Sinigaglia. 1995. Peptide binding specificity of HLA-DR4 molecules: correlation with rheumatoid arthritis association. *J. Exp. Med.* 181: 1847–1855.
11. Scally, S. W., J. Petersen, S. C. Law, N. L. Dudek, H. J. Nel, K. L. Loh, L. C. Wijeyewickrema, S. B. G. Eckle, J. van Heemst, R. N. Pike, et al. 2013. A molecular basis for the association of the HLA-DRB1 locus, citrullination, and rheumatoid arthritis. *J. Exp. Med.* 210: 2569–2582.
12. van Heemst, J., D. van der Woude, T. W. Huizinga, and R. E. Toes. 2014. HLA and rheumatoid arthritis: how do they connect? *Ann. Med.* 46: 304–310.
13. De Almeida, D. E., S. Ling, X. Pi, A. M. Hartmann-Scruggs, P. Pumpens, and J. Holoshitz. 2010. Immune dysregulation by the rheumatoid arthritis shared epitope. *J. Immunol.* 185: 1927–1934.
14. Fu, J., S. Ling, Y. Liu, J. Yang, S. Naveh, M. Hannah, C. Gilon, Y. Zhang, and J. Holoshitz. 2013. A small shared epitope-mimetic compound potently accelerates osteoclast-mediated bone damage in autoimmune arthritis. *J. Immunol.* 191: 2096–2103.
15. Holoshitz, J., Y. Liu, J. Fu, J. Joseph, S. Ling, A. Colletta, P. Sharma, D. Begun, S. Goldstein, and R. Taichman. 2013. An HLA-DRB1-coded signal transduction ligand facilitates inflammatory arthritis: a new mechanism of autoimmunity. *J. Immunol.* 190: 48–57.
16. Ling, S., A. Cheng, P. Pumpens, M. Michalak, and J. Holoshitz. 2010. Identification of the rheumatoid arthritis shared epitope binding site on calreticulin. *PLoS One* 5: e11703.

17. Ling, S., A. Lai, O. Borschukova, P. Pumpens, and J. Holoshitz. 2006. Activation of nitric oxide signaling by the rheumatoid arthritis shared epitope. *Arthritis Rheum.* 54: 3423–3432.
18. Ling, S., Z. Li, O. Borschukova, L. Xiao, P. Pumpens, and J. Holoshitz. 2007. The rheumatoid arthritis shared epitope increases cellular susceptibility to oxidative stress by antagonizing an adenosine-mediated anti-oxidative pathway. *Arthritis Res. Ther.* 9: R5.
19. Ling, S., X. Pi, and J. Holoshitz. 2007. The rheumatoid arthritis shared epitope triggers innate immune signaling via cell surface calreticulin. *J. Immunol.* 179: 6359–6367.
20. Pan, S., T. Trejo, J. Hansen, M. Smart, and C. S. David. 1998. HLA-DR4 (DRB1*0401) transgenic mice expressing an altered CD4-binding site: specificity and magnitude of DR4-restricted T cell response. *J. Immunol.* 161: 2925–2929.
21. Taneja, V., N. Taneja, M. Behrens, S. Pan, T. Trejo, M. Griffiths, H. Luthra, and C. S. David. 2003. HLA-DRB1*0402 (DW10) transgene protects collagen-induced arthritis-susceptible H2Aq and DRB1*0401 (DW4) transgenic mice from arthritis. *J. Immunol.* 171: 4431–4438.
22. Zendman, A. J., R. Raijmakers, S. Nijenhuis, E. R. Vossenaar, M. Tillaart, R. G. Chirivi, J. M. Raats, W. J. van Venrooij, J. W. Drijfhout, and G. J. Pruijn. 2007. ABAP: antibody-based assay for peptidylarginine deiminase activity. *Anal. Biochem.* 369: 232–240.
23. Goicoechea, S., A. W. Orr, M. A. Pallero, P. Eggleton, and J. E. Murphy-Ullrich. 2000. Thrombospondin mediates focal adhesion disassembly through interactions with cell surface calreticulin. *J. Biol. Chem.* 275: 36358–36368.
24. Endo, M., S. Oyadomari, M. Suga, M. Mori, and T. Gotoh. 2005. The ER stress pathway involving CHOP is activated in the lungs of LPS-treated mice. *J. Biochem.* 138: 501–507.
25. Liang, S. H., W. Zhang, B. C. McGrath, P. Zhang, and D. R. Cavener. 2006. PERK (eIF2alpha kinase) is required to activate the stress-activated MAPKs and induce the expression of immediate-early genes upon disruption of ER calcium homoeostasis. *Biochem. J.* 393: 201–209.
26. Martinon, F., X. Chen, A. H. Lee, and L. H. Glimcher. 2010. TLR activation of the transcription factor XBP1 regulates innate immune responses in macrophages. *Nat. Immunol.* 11: 411–418.
27. Panaretakis, T., O. Kepp, U. Brockmeier, A. Tesniere, A. C. Bjorklund, D. C. Chapman, M. Durchschlag, N. Joza, G. Pierron, P. van Endert, et al. 2009. Mechanisms of pre-apoptotic calreticulin exposure in immunogenic cell death. *EMBO J.* 28: 578–590.
28. Darrah, E., A. Rosen, J. T. Giles, and F. Andrade. 2012. Peptidylarginine deiminase 2, 3 and 4 have distinct specificities against cellular substrates: novel insights into autoantigen selection in rheumatoid arthritis. *Ann. Rheum. Dis.* 71: 92–98.
29. Tutturen, A. E., B. Fleckenstein, and G. A. de Souza. 2014. Assessing the citrullinome in rheumatoid arthritis synovial fluid with and without enrichment of citrullinated peptides. *J. Proteome Res.* 13: 2867–2873.
30. Vossenaar, E. R., T. R. Radstake, A. van der Heijden, M. A. van Mansum, C. Dieteren, D. J. de Rooij, P. Barrera, A. J. Zendman, and W. J. van Venrooij. 2004. Expression and activity of citrullinating peptidylarginine deiminase enzymes in monocytes and macrophages. *Ann. Rheum. Dis.* 63: 373–381.
31. Teitelbaum, S. L. 2006. Osteoclasts; culprits in inflammatory osteolysis. *Arthritis Res. Ther.* 8: 201.
32. Van Linthoudt, D., L. Malterre, C. Bernet, and A. Pazera. 2002. Isolated asymmetrical acro-osteolysis of the big toe in an elder patient with rheumatoid arthritisasymmetrical. *Joint Bone Spine* 69: 340–342.
33. Seri, Y., H. Shoda, A. Suzuki, I. Matsumoto, T. Sumida, K. Fujio, and K. Yamamoto. 2015. Peptidylarginine deiminase type 4 deficiency reduced arthritis severity in a glucose-6-phosphate isomerase-induced arthritis model. *Sci. Rep.* 5: 13041.
34. Harre, U., D. Georgess, H. Bang, A. Bozec, R. Axmann, E. Ossipova, P. J. Jakobsson, W. Baum, F. Nimmerjahn, E. Szarka, et al. 2012. Induction of osteoclastogenesis and bone loss by human autoantibodies against citrullinated vimentin. *J. Clin. Invest.* 122: 1791–1802.
35. Raychaudhuri, S., C. Sandor, E. A. Stahl, J. Freudenberg, H. S. Lee, X. Jia, L. Alfredsson, L. Padyukov, L. Klareskog, J. Worthington, et al. 2012. Five amino acids in three HLA proteins explain most of the association between MHC and seropositive rheumatoid arthritis. *Nat. Genet.* 44: 291–296.
36. van Heemst, J., T. J. W. Huizinga, D. van der Woude, and R. E. M. Toes. 2015. Fine-mapping the human leukocyte antigen locus in rheumatoid arthritis and other rheumatic diseases: identifying causal amino acid variants? *Curr. Opin. Rheumatol.* 27: 256–261.
37. de Almeida, D. E., and J. Holoshitz. 2011. MHC molecules in health and disease: at the cusp of a paradigm shift. *Self Nonself* 2: 43–48.
38. Holoshitz, J. 2013. The quest for better understanding of HLA-disease association: scenes from a road less travelled by. *Discov. Med.* 16: 93–101.
39. Alsaleh, G., G. Suffert, N. Semaan, T. Juncker, L. Frenzel, J. E. Gottenberg, J. Sibilia, S. Pfeffer, and D. Wachsmann. 2009. Bruton's tyrosine kinase is involved in miR-346-related regulation of IL-18 release by lipopolysaccharide-activated rheumatoid fibroblast-like synoviocytes. *J. Immunol.* 182: 5088–5097.
40. Esquivel, P. S., N. R. Rose, and Y. C. Kong. 1977. Induction of autoimmunity in good and poor responder mice with mouse thyroglobulin and lipopolysaccharide. *J. Exp. Med.* 145: 1250–1263.
41. Vatanen, T., A. D. Kostic, E. d'Hennezel, H. Siljander, E. A. Franzosa, M. Yassour, R. Kolde, H. Vlamakis, T. D. Arthur, A. M. Hämäläinen, et al; DIABIMMUNE Study Group. 2016. Variation in microbiome LPS immunogenicity contributes to autoimmunity in humans. [Published erratum appears in 2016 *Cell* 165: 1551.] *Cell* 165: 842–853.